Check for updates

High Power Laser Science and Engineering, (2025), Vol. 13, e68, 8 pages.
doi:10.1017/hpl.2025.10047

HIGH POWER LASER SCIENCE AND ENGINEERING

RESEARCH ARTICLE

Impact of imperfect surface and imperfect groove pattern of compressor diffraction gratings on laser pulse focal intensity

Efim Khazanov

Gaponov-Grekhov Institute of Applied Physics, Russian Academy of Sciences, Nizhny Novgorod, Russia

(Received 22 January 2025; revised 8 May 2025; accepted 19 June 2025)

Abstract

An analytical expression for focal intensity is derived for arbitrary surface profiles and arbitrary groove patterns of compressor gratings. The expression is valid for different compressor designs: plane and out-of-plane compressors, symmetric and asymmetric compressors (compressors composed by two not-identical pairs of gratings) and a two-grating compressor. It is shown that the quality requirements for the optics used to write a grating are higher than for the grating. The focal intensity can be maximized by rotating each grating around its normal by 180 degrees. Moreover, it may be increased to maximum by interchanging any two gratings in the compressor, because imperfections of an individual grating do not additively affect the focal intensity. The intensity decrease is proportional to the squared pulse spectrum width and the squared total distortions of the second and third gratings of the four-grating compressor and the total distortions of two gratings of the two-grating compressor.

Keywords: femtosecond lasers; groove patterns of diffraction gratings; out-of-plane compressors

1. Introduction

The compressor in chirped pulse amplification lasers is one of the key elements of all high-power femtosecond lasers[1,2]. Its main function is to compress the pulse to the Fourier limit, that is, to obtain a pulse with a constant spectral phase at the output. In practice, an inevitable residual spectral phase is still crucial. To approach the Fourier limit, an acousto-optic programmable dispersive filter (AOPDF)[3] is used. The shortest pulse is a key goal, because it provides the highest pulse power for a given pulse energy. Nevertheless, the most important parameter is the focal intensity, which strongly depends on beam focusability. The highest focusability is provided by a diffraction limited beam, that is, a beam with a plane wavefront (a flat spatial phase). To approach the diffraction limited beam, adaptive mirrors (AMs) are widely employed[4]. The AOPDF and AM efficiently correct temporal and spectral phase distortions separately, but they are not able to compensate for space–time coupling; therefore, the focal intensity is less than the diffraction limit. Besides the reduction of focal intensity (which is the subject of the present paper), the space–time coupling affects the pulse contrast ratio. The contrast degradation due to imperfect surface quality of stretcher and compressor optics has been studied analytically[5–7], numerically[8–11] and experimentally[7,10,11].

Compressor diffraction gratings introduce two types of space–time coupling: amplitude and phase. The amplitude coupling is related to the spatial dependence of the reflection coefficient[12], as well as to the beam clipping on the gratings[12,13], if any. In this paper, we will restrict our study to the phase space–time coupling caused by two reasons. The first one is an imperfectly flat grating surface. This effect was numerically studied in Refs. [12, 14–20], and an analytical expression for the focal intensity for arbitrary compressor grating surface profiles was obtained in Ref. [21].

The second, much less studied, reason for the phase space–time coupling is the groove pattern imperfection: non-equidistance and non-parallelism. In this case, the wavefront of the wave reflected from the grating is no longer flat, even for a perfectly flat surface, and the wavefront distortions are different for different frequencies, which results in space–time coupling. Methods for measuring groove imperfection of the grating were proposed in Refs. [22, 23]. For

Correspondence to: E. Khazanov, Gaponov-Grekhov Institute of Applied Physics, Russian Academy of Sciences, Nizhny Novgorod 603950, Russia. Email: efimkhazanov@gmail.com

© The Author(s), 2025. Published by Cambridge University Press in association with Chinese Laser Press. This is an Open Access article, distributed under the terms of the Creative Commons Attribution-NonCommercial licence (https://creativecommons.org/licenses/by-nc/4.0), which permits non-commercial re-use, distribution, and reproduction in any medium, provided the original article is properly cited. The written permission of Cambridge University Press must be obtained prior to any commercial use.

https://doi.org/10.1017/hpl.2025.10047 Published online by Cambridge University Press

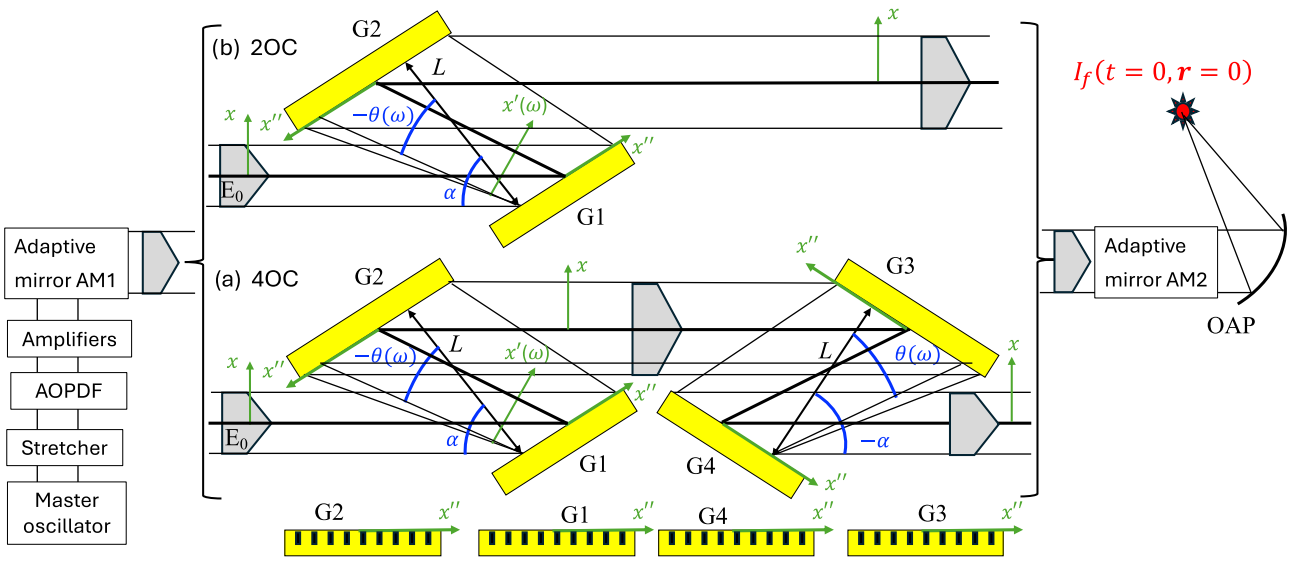

Figure 1. 4OC (symmetric) (a) and 2OC (maximum asymmetric) (b). G1–G4, gratings; OAP, off-axis parabola; $m=-1$; the angle of reflection from the first grating is negative. Angle γ is not shown as it is outside the plane of the figure; γ is the same for all gratings.

holographic gratings, groove imperfection is determined exclusively by the imperfect wavefronts of the waves used for writing the grating[24,25]. The impact of groove imperfection on the compressor of femtosecond laser pulses was studied in Ref. [24], where only a particular case of period-chirped gratings was considered. The simplest case in which only the fourth grating of the classical Treacy compressor (TC)[26] is non-ideal was studied analytically in Ref. [23]. The TC consists of two identical pairs of diffraction gratings, where the gratings in each pair are parallel and the pairs are mirror images of each other, that is, the TC is a plane symmetric compressor.

Recently, two routes of TC modification have been discussed in the literature. The first one – an asymmetric compressor – is based on abandoning symmetry, and the second – an out-of-plane compressor (OC) – is based on abandoning flat geometry. In the asymmetric compressor proposed in Ref. [27] two pairs of parallel diffraction gratings differ from each other by grating distance and/or incident angle. An important property of the asymmetric compressor is smoothing of fluence fluctuations, which allows a significant reduction of the probability of optical breakdown of the fourth grating. In Ref. [28], an analytical theory was constructed, which showed that no compressor asymmetry reduces focal intensity. This conclusion is also true for a compressor consisting of one pair of gratings, which is a special (maximum asymmetric) case[12,29,30]. In the OC[31–38], the angle of incidence in the plane normal to the diffraction plane is nonzero. In Ref. [39] it was shown that effective smoothing of the output beam is also possible in the OC, which was confirmed experimentally[40]. In Ref. [41] it was proposed to use the OC to increase the output power by reducing the angle of incidence.

In Section 2, the focal intensity will be found analytically for an arbitrary symmetric OC and a maximum asymmetric OC consisting of one pair of gratings. The influence of the grating surface profile imperfection will be compared with the impact of the groove pattern imperfection, and the symmetric compressor will be compared with the asymmetric one and the plane compressor with the OC in Section 3.

2. Dependence of focal intensity on out-of-plane compressor parameters

Let the compressor consist of gratings with groove density N and distance between the gratings along the normal L. We will consider the OC with the angle of incidence on the first grating α in the diffraction plane and γ in the non-diffraction plane. Most labs use a compressor consisting of two identical pairs of gratings: the parameters α, γ, N and L are the same for the two pairs. Such a compressor is referred to as a symmetric one (Figure 1(a)). In an asymmetric compressor[27,28,39,42] the grating pairs differ from each other; they have at least one of the parameters α, γ, N or L that differs from the others. The asymmetric compressor smooths small-scale fluence fluctuations and, hence, reduces the probability of laser-induced damage. A special case of the asymmetric compressor is a compressor consisting of just one pair of gratings – a two-grating compressor (Figure 1(b))[13,27,30]. It has some additional advantages: smoothing of large-scale fluence fluctuations, simplicity and lower cost. From the point of view of compressor (a)symmetry, we will restrict ourselves to two most interesting cases – a symmetric compressor and an asymmetric two-grating compressor (Figures 1(a) and 1(b)). They will be designated as 4OC (four-grating OC) and 2OC (two-grating OC). A plane

https://doi.org/10.1017/hpl.2025.10047 Published online by Cambridge University Press

TC is a particular case of the OC at $\gamma = 0$, so it will be designated as 4TC and 2TC. Another interesting special case is the Littrow compressor, in which $\alpha = \alpha_L$, where α_L is the Littrow angle; the abbreviations 4LC and 2LC will be used for this compressor. The LC has a number of additional advantages[21,33,41]. We assume that the beam size and the size of gratings G2 and G3 are such that all frequencies fall into the aperture of G2 and G3, that is, there are no beams that 'miss' the grating. This is not the case for the so-called full-aperture compressor [13,30,43], which is not considered in this paper.

In the case of a perfect grating, the incident plane wave after reflection remains plane, that is, its spatial phase $\Delta(x,y) = \text{const}$, and the angle of reflection $\theta(\omega)$ is determined by the following expression for the grating:

$$\sin\theta(\omega) = m\frac{2\pi c}{\omega}\frac{N}{\cos\gamma} + \sin\alpha, \tag{1}$$

where m is the diffraction order. A perfect grating is understood as a grating with a perfectly flat substrate surface and perfectly parallel and equidistant grooves. As a result of an imperfect (out-of-plane) surface and imperfect (non-equidistant and non-parallel) grooves, the wavefront of the reflected wave is no longer flat and $\Delta(x,y) \neq \text{const}$. AM1,2 can compensate for distortions only at one (central) frequency ω_0. Since Δ depends on frequency ω (space–time coupling), this compensation cannot be complete, which leads to a decrease in the focal intensity. In Ref. [23], an expression was found for the spatial phase $\Delta(x',y',\omega)$ of a plane monochromatic wave after reflection from the grating:

$$\Delta(x',y',\omega) = -\frac{\omega}{c}\left(H_{gr}h_{gr}\left(\frac{x'}{\cos\theta(\omega)},\frac{y'}{\cos\gamma}\right) + H_{wr}h_{wr}\left(\frac{x'\cos\Phi}{\cos\theta(\omega)},\frac{y'}{\cos\gamma}\right)\right), \tag{2}$$

where

$$H_{gr}(\omega) = \cos\gamma\,(\cos\alpha + \cos\theta(\omega)),\ H_{wr}(\omega) = 2\frac{\omega_{wr}}{\omega}, \tag{3}$$

where $h_{gr}(x'',y'')$ is the profile of the grating surface; $h_{wr}(x'',y'')$ characterizes groove pattern imperfection and has the sense of the difference of the total surface profiles of the optical elements on the path of two waves writing the holographic grating (Figure 2); $\omega_{wr} = 2\pi c/\lambda_{wr}$ is the frequency of the writing waves; and Φ is the angle of incidence of the writing waves on the grating substrate, $\sin\Phi = N\lambda_{wr}/2$. Here, (x'',y'') are the coordinates of the grating surface and (x',y') are the coordinates in the plane normal to the wave vector of the beam between the first and second gratings shown in Figure 1. On reflection from the second grating, the beam changes its size, that is, to pass to the laboratory reference frame, (x,y), x' in Equation (2) must be replaced by $\frac{\cos\theta(\omega)}{\cos\alpha}x$. Thus, the phase introduced into the beam upon reflection from the first grating has the following form:

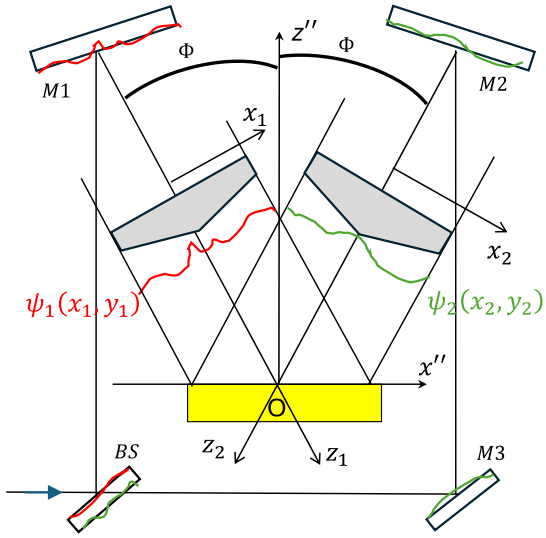

Figure 2. Scheme of writing a holographic grating. BS, beamsplitter; M1–M3, mirrors; $\psi_{1,2}$, phase of the beams writing the grating; $\psi_1 - \psi_2 = 2k_{wr}h_{wr}$.

$$\Delta_1(x,y,\omega) = -\frac{\omega}{c}\left(H_{gr}h_{gr,1}\left(\frac{x}{\cos\alpha},\frac{y}{\cos\gamma}\right) + H_{wr}h_{wr,1}\left(\frac{x\cos\Phi}{\cos\alpha},\frac{y}{\cos\gamma}\right)\right). \tag{4}$$

To find the phase for the remaining gratings, we fix the coordinate system (x'',y'') on each grating (Figure 1) so that, in the case of identical gratings, the functions $h_{gr}(x'',y'')$ and $h_{wr}(x'',y'')$ should be identical for all gratings: $h_{gr} = h_{gr,n}; h_{wr} = h_{wr,n}; n = 1,2,3,4$ is the grating number.

As can be seen from Figure 1, for even gratings the angle between the x''- and x-axes is obtuse; therefore, the sign of the first argument in h_{gr} and h_{wr} for them should be changed: $x \to -x$. Accordingly, for a grating with number n, the substitution $x \to (-1)^{n+1}x$ should be made on the right-hand side of Equation (4). As shown in Ref. [23], the expression in Equation (2) is valid if the wave vector of the incident wave makes an acute angle with the x''-axis. If this angle is obtuse, then the plus sign in front of H_{wr} should be replaced with the minus sign. From Figure 1 it is clear that G3 and G4 must have the minus sign. Therefore, in front of H_{wr} the factor $(-1)^{\left[\frac{n-1}{2}\right]}$ should be used, where $[\ldots]$ denotes the integer part. In addition, for the second and fourth gratings in Equation (2), obvious substitutions $\alpha \to -\theta(\omega)$ and $\theta(\omega) \to -\alpha$ should be made. Taking all this into account, the phase introduced by the reflection from

https://doi.org/10.1017/hpl.2025.10047 Published online by Cambridge University Press

the grating with number n takes on the following form:

$$\Delta_n(x,y,\omega) = -\frac{\omega}{c}\left(H_{\mathrm{gr}}h_{\mathrm{gr},n}\left((-1)^{n+1}\frac{x}{\cos\alpha},\frac{y}{\cos\gamma}\right) + (-1)^{\left[\frac{n-1}{2}\right]}H_{\mathrm{wr}}h_{\mathrm{wr},n}\left((-1)^{n+1}\frac{x\cos\Phi}{\cos\alpha},\frac{y}{\cos\gamma}\right)\right). \quad (5)$$

Let the input field have the following form:

$$E_0(\omega,\boldsymbol{r}) = e^{i\varphi_{\mathrm{in}}(\omega)+i\varphi_{\mathrm{D}}(\omega)}e^{-\left(\frac{\omega-\omega_0}{\Delta\omega}\right)^{2\mu}}e^{iy\frac{\omega}{c}\sin\gamma}\left|E_0(\boldsymbol{r})\right|, \quad (6)$$

where $\varphi_{\mathrm{in}}(\omega)$ is the spectral phase without allowance for the phase introduced by the AOPDF $\varphi_{\mathrm{D}}(\omega)$. Here we assume that the wavefront of $E_0(\boldsymbol{r})$ is plane, that is, $E_0(\boldsymbol{r}) = |E_0(\boldsymbol{r})|$. If this is not the case, AM1 can fix it. The Strehl ratio is defined by the following:

$$St = \frac{I_{\mathrm{f}}}{I_{\mathrm{f}}\left(h_{\mathrm{gr}} = h_{\mathrm{wr}} = 0\right)}, \quad (7)$$

where I_{f} is focal intensity. According to Equation (7), the Strehl ratio shows the reduction of the focal intensity compared to the case of compressor gratings with a perfectly plane surface and perfectly parallel and equidistant grooves. We assume that AM2 provides a plane wavefront at central frequency ω_0, and AOPDF ensures a constant spectral phase at zero spatial frequency $\kappa = 0$, as under these conditions I_{f} is maximal[21]. Following the procedure described in Ref. [21], in the $\left(\frac{\Delta\omega}{\omega_0}\right)^2\overline{\Psi_{4,2}^2} \ll 2$ approximation for 4OC and 2OC we find St_2 and St_4:

$$St_{4,2} = 1 - M(\mu)\left(\frac{\Delta\omega}{\omega_0}\right)^2\overline{\Psi_{4,2}^2(x,y)}, \quad (8)$$

where $M(\mu) = \Gamma\left(\frac{3}{2\mu}\right)/\Gamma\left(\frac{1}{2\mu}\right)$, Γ is the gamma function and $\overline{(\dots)}$ denotes averaging over the grating surface with the weight of the laser field module:

$$\overline{(\dots)} \equiv \frac{\int |E_0(x\cos\alpha, y\cos\gamma)|\,(\dots)\,\mathrm{d}x\mathrm{d}y}{\int |E_0(x\cos\alpha, y\cos\gamma)|\,\mathrm{d}x\mathrm{d}y}, \quad (9)$$

$$\Psi_4(x,y) = fg_4(x,y) + uw_4(x\cos\Phi, y) - \mathbf{FG}(x,y) - \mathbf{UW}(x\cos\Phi, y), \quad (10)$$

$$\Psi_2(x,y) = fg(x,y) + uw(x\cos\Phi, y), \quad (11)$$

$$g_4(x,y) = \sum_{n=1}^{4} h_{\mathrm{gr},n}\left((-1)^{n+1}x, y\right),$$
$$w_4(x,y) = \sum_{n=1}^{4}(-1)^{\left[\frac{n-1}{2}\right]}h_{\mathrm{wr},n}\left((-1)^{n+1}x, y\right), \quad (12)$$

$$g(x,y) = h_{\mathrm{gr},1}(x,y) + h_{\mathrm{gr},2}(-x,y),$$
$$w(x,y) = h_{\mathrm{wr},1}(x,y) + h_{\mathrm{wr},2}(-x,y), \quad (13)$$

$$\mathbf{G}(x,y) = \nabla h_{\mathrm{gr},2}(-x,y) + \nabla h_{\mathrm{gr},3}(x,y),$$
$$\mathbf{W}(x,y) = -\nabla h_{\mathrm{wr},2}(-x,y) - \nabla h_{\mathrm{wr},3}(x,y), \quad (14)$$

$$f = 2\pi N\mathrm{tg}\beta, \quad u = \frac{4\pi}{\lambda_{\mathrm{wr}}},$$
$$\mathbf{F} = 2\pi NL\frac{\cos\alpha+\cos\beta}{\cos\gamma\cos^3\beta}\begin{pmatrix}\cos\alpha\cos\gamma\\ \lambda_0 N\mathrm{tg}\gamma\end{pmatrix},$$
$$\mathbf{U} = 2\frac{\mathrm{tg}\left(\frac{\alpha-\beta}{2}\right)}{N\lambda_{\mathrm{wr}}}\mathbf{F}, \quad (15)$$

$$\nabla h(-x,y) \triangleq \nabla h(x,y)|_{x=-x}, \quad (16)$$

where $\beta = \theta(\omega_0)$. Hereafter, the sub-indices '2' and '4' correspond to the two-grating (Figure 1(b)) and the four-grating (Figure 1(a)) compressors. The sub-index '4, 2' denotes either the four-grating or the two-grating compressor. Without loss of generality, hereinafter we assume that $\overline{g} = \overline{w} = \overline{g_4} = \overline{w_4} = \overline{\boldsymbol{G}} = \overline{\mathbf{W}} = 0$. In addition, the functions $h_{\mathrm{gr},n}$ and $h_{\mathrm{wr},n}$ do not contain components linear with respect to x and y (wedges) that are equivalent to the rotation of the grating as a whole for $h_{\mathrm{gr},n}$ and to the changes in the groove density N uniformly over the entire grating surface for $h_{\mathrm{wr},n}$. As shown in Ref. [21], all the components in $\nabla h_{\mathrm{gr},n}(x,y)$ linear with respect to x and y can be effectively compensated for by rotating one grating, for example, G4. The same is true for $\nabla h_{\mathrm{wr},n}(x,y)$. If this is done, then the terms linear with respect to x and y should be subtracted from $\nabla h_{\mathrm{gr},n}(x,y)$ and $\nabla h_{\mathrm{wr},n}(x,y)$ in Equation (14). These terms correspond to the aberrations of $h_{\mathrm{gr},n}(x,y)$ and $h_{\mathrm{wr},n}(x,y)$ quadratic with respect to x and y, that is, to defocus, vertical astigmatism and oblique astigmatism.

Taking into account that $|\nabla h_n(x,y)| \approx \frac{h_n(x,y)}{d}$, where $d < \frac{L_{\mathrm{g}}}{2}$ is a typical transverse scale of $h_i(x,y)$ variation, and that $L_{\mathrm{g}} < L$, we obtain the following:

$$\frac{fg_4(x,y)}{\mathbf{FG}(x,y)} \preccurlyeq \frac{\sin\beta\cos^2\beta}{2(\cos\alpha+\cos\beta)\cos\alpha}\frac{L_{\mathrm{g}}}{L} \ll 1,$$
$$\frac{uw_4}{\mathbf{UW}} \preccurlyeq \frac{\mathrm{ctg}\left(\frac{\alpha-\beta}{2}\right)\cos^3\beta}{2(\cos\alpha+\cos\beta)\cos\alpha}\frac{L_{\mathrm{g}}}{L} \ll 1, \quad (17)$$

and the expression in Equation (10) reduces to the following:

$$\Psi_4(x,y) = -\frac{\omega_0}{c}\left(\mathbf{FG}(x,y) + \mathbf{UW}(x\cos\Phi, y)\right). \quad (18)$$

Let us now consider this case and use Equation (18) for 4OC. It should be noted, however, that the above

https://doi.org/10.1017/hpl.2025.10047 Published online by Cambridge University Press

approximation is violated if the quadratic components in $h_{\mathrm{gr},n}(x,y)$ and $h_{\mathrm{wr},n}(x,y)$ are significantly larger than all the others taken together. Then, if the quadratic distortions are compensated for by rotating the fourth grating[21], the approximation $|\nabla h_n(x,y)| \approx \frac{h_n(x,y)}{d}$ is invalid and Equation (10) must be used instead of Equation (18).

As seen from Equation (18), the focal intensity for 4OC is determined by the total value of the h_{gr} and h_{wr} gradients (functions $\mathbf{G}(x,y)$ and $\mathbf{W}(x,y)$), where only gratings G2 and G3 are significant, whereas the contribution of G1 and G4 is negligible. Contrariwise, for 2OC, according to Equation (11), the gradients are of no importance, and the focal intensity is determined only by the total values of h_{gr} and h_{wr} (functions $g(x,y)$ and $w(x,y)$).

Analogous to Equation (17), we obtain $fg(x,y) \ll \mathbf{FG}(x,y)$ and $uw(x,y) \ll \mathbf{U}\boldsymbol{W}(x,y)$. With allowance for Equations (11) and (18), this follows that a decrease in the Strehl ratio in 2OC is much smaller than in 4OC: $(1-St_2) \ll (1-St_2)$, which is a significant advantage of the two-grating compressor along with its other merits[21,33,41].

3. Discussion of results

As can be seen from Equation (8), one function $\Psi_{4,2}(x,y)$ is responsible for all distortions of all compressor gratings. It has the meaning of the effective phase (effective wavefront), which characterizes all imperfections of all compressor gratings. The decrease in the Strehl ratio $\left(1-St_{4,2}\right)$ is proportional to the squared root mean square (rms) of this phase and to the squared $\Delta\omega$. Therefore, a decrease/increase in $\Delta\omega$ proportionally reduces/increases the requirements for the rms of both the surface of the gratings and the surfaces of the optics used for their writing. To determine the Strehl ratio it is sufficient to know only $\overline{\Psi_{4,2}^2(x,y)}$, that is, the dispersion (rms squared) of the function $\Psi_{4,2}(x,y)$, with averaging being performed according to Equation (9). The laser beam profile $E_0(x,y)$ affects $St_{4,2}$ only through this averaging. It is obvious that the flat-top profile is better than the Gaussian one, especially in the presence in $\Psi_{4,2}(x,y)$ of Zernike polynomials with large radial indices. The pulse spectrum profile has a similar effect: for a Gaussian spectrum $M(\mu=1)=0.5$ and for $\mu \geq 6, M \approx 0.32$, that is, for a super-Gaussian spectrum, $St_{4,2}$ is larger than for a Gaussian one.

The function $\Psi_{4,2}(x,y)$ is determined by the total distortions of gratings G2 and G3 for 4OC (Equation (14)) and G1 and G2 for 2OC (Equation (13)). The rotation of one grating by 180 degrees around its normal changes the sign of the arguments of the functions $h_{\mathrm{gr}}(x,y)$ and $h_{\mathrm{wr}}(x,y)$. In addition, with such a rotation, the angle between the wave vector of the incident wave and the x''-axis changes from acute to obtuse or vice versa, that is, $h_{\mathrm{wr},n}(x,y)$ changes its sign[23]. Thus, the rotation corresponds to the replacements:

$$h_{\mathrm{gr},n}(x,y) \to h_{\mathrm{gr},n}(-x,-y) \text{ and}$$
$$h_{\mathrm{wr},n}(x,y) \to -h_{\mathrm{wr},n}(-x,-y). \tag{19}$$

In 2OC the gratings may be arranged in four non-equivalent ways: each grating may be placed in two ways. There are significantly more options in 4OC. The values of $\overline{\Psi_{4,2}^2(x,y)}$ and, hence, of $St_{4,2}$ will be different for different variants. Knowing $h_{\mathrm{gr},n}(x,y)$ and $h_{\mathrm{wr},n}(x,y)$ for each grating, for any compressor it is easy to choose the best option – the one that gives the smallest value of $\overline{\Psi_{4,2}^2(x,y)}$.

The grating surface profiles $h_{\mathrm{gr},n}(x,y)$ are, as a rule, independent for different gratings. In contrast, it is reasonable to conjecture that $h_{\mathrm{wr},n}(x,y) = h_{\mathrm{wr}}(x,y)$, if the gratings are written by the same optics (see Figure 2). Then, from Equations (13) and (14) we obtain the following:

$$w(x,y) = h_{\mathrm{wr}}(x,y) + h_{\mathrm{wr}}(-x,y),$$
$$\mathbf{W}(x,y) = -\nabla h_{\mathrm{wr}}(-x,y) - \nabla h_{\mathrm{wr}}(x,y), \tag{20}$$

that is, the Zernike polynomials that are odd in x will make a zero contribution to $w(x,y)$, and even ones a zero contribution to $\mathbf{W}(x,y)$ (see Equation (16)). If the second grating is rotated by 180 degrees around its normal, then we have the following:

$$w(x,y) = h_{\mathrm{wr}}(x,y) - h_{\mathrm{wr}}(x,-y),$$
$$\mathbf{W}(x,y) = -\nabla h_{\mathrm{wr}}(-x,y) + \nabla h_{\mathrm{wr}}(-x,-y), \tag{21}$$

and the Zernike polynomials that are even in y will make a zero contribution to $w(x,y)$, and the odd ones to $\mathbf{W}(x,y)$. From this it is clear that identical gratings do not allow for compensating for the imperfection of the grooves of each other, since in any case $w(x,y) \neq 0$ and $\mathbf{W}(x,y) \neq 0$. However, $w(x,y) = 0$ if any of the conditions

$$h_{\mathrm{wr},2}(x,y) = -h_{\mathrm{wr},1}(-x,y) \text{ or}$$
$$h_{\mathrm{wr},2}(x,y) = h_{\mathrm{wr},1}(x,-y) \tag{22}$$

is met, and $\mathbf{W}(x,y) = 0$ if any of the conditions

$$\nabla h_{\mathrm{wr},2}(x,y) = -\nabla h_{\mathrm{wr},1}(-x,y) \text{ or}$$
$$\nabla h_{\mathrm{wr},2}(-x,-y) = \nabla h_{\mathrm{wr},1}(-x,y) \tag{23}$$

is fulfilled. Thus, to completely nullify the influence of an imperfect groove pattern for 2OC or 4OC, a pair of grooves satisfying Equation (22) or (23), respectively, should be written. By interchanging the beamsplitter (BS) and M3, as well as M1 and M2 (Figure 2), it is possible to change the sign of h_{wr}, but this is insufficient to fulfill Equations (22) and (23).

https://doi.org/10.1017/hpl.2025.10047 Published online by Cambridge University Press

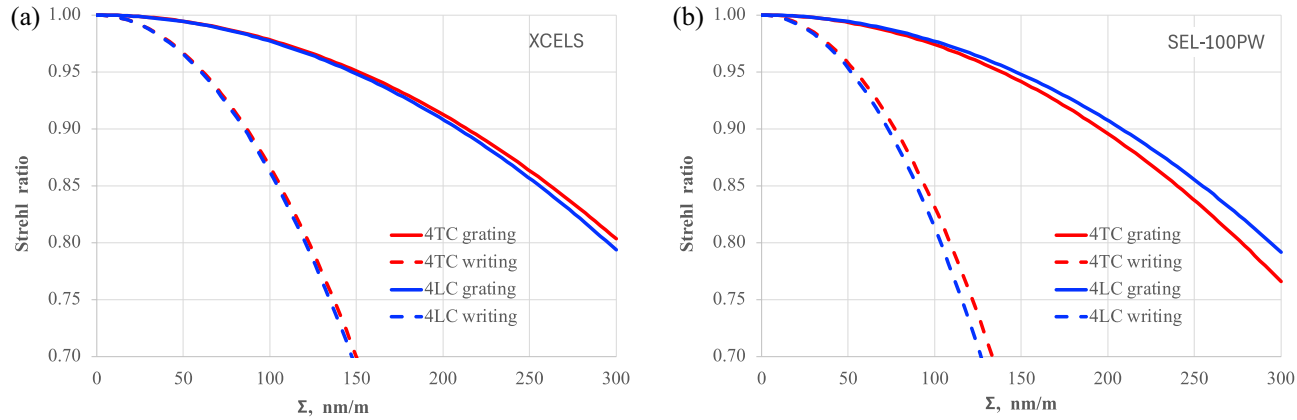

Figure 3. Here, $St_{4,\mathrm{gr}}(\Sigma)$ (solid curves) and $St_{4,\mathrm{wr}}(\Sigma)$ (dashed curves) are plotted by Equation (25) for 4TC (red) and 4LC (blue) for the compressor parameters (see Table 1) proposed for XCELS (a) and SEL-100PW (b).

Table 1. Compressor parameters.

	XCELS 910±75 nm		SEL-100PW 925±100 nm	
	4TC	4LC	4TC	4LC
N, mm^{-1}	950	1000	1000	1100
α, degree	36	27.4	38.5	31.3
γ, degree	0	11.2	0	14.8
L, cm	333	231	272	155

The Strehl ratio St depends on (i) the total grating profile described by the functions $\mathbf{G}(x,y)$ and $g(x,y)$ and (ii) the total groove imperfection which, in turn, is determined by the total profile of the optics used for writing the grooves that is described by the functions $\mathbf{W}(x,y)$ and $w(x,y)$. Compare the influence of these two reasons assuming that the profiles are uncorrelated, that is, $\overline{\mathbf{GW}} = \overline{gw} = 0$. Then, from Equations (8), (11) and (18) we find that the Strehl ratio St is a product of the Strehl ratio caused by the grating surface imperfection St_{gr} and the Strehl ratio caused by the groove pattern imperfection St_{wr}:

$$St_4 = St_{4,\mathrm{gr}} St_{4,\mathrm{wr}}, \quad St_2 = St_{2,\mathrm{gr}} St_{2,\mathrm{wr}}, \tag{24}$$

$$St_{4,\mathrm{gr}} = 1 - M\left(\frac{\Delta\omega}{\omega_0}\right)^2 \left(F_x^2\overline{G_x^2} + F_y^2\overline{G_y^2}\right),$$
$$St_{4,\mathrm{wr}} = 1 - M\left(\frac{\Delta\omega}{\omega_0}\right)^2 \left(U_x^2\overline{W_x^2} + U_y^2\overline{W_y^2}\right), \tag{25}$$

$$St_{2,\mathrm{gr}} = 1 - M\left(\frac{\Delta\omega}{\omega_0}\right)^2 f^2\overline{g^2},$$
$$St_{2,\mathrm{wr}} = 1 - M\left(\frac{\Delta\omega}{\omega_0}\right)^2 u^2\overline{w^2}. \tag{26}$$

Note that for the St close to unity, the contribution of these two factors to the reduction of the Strehl ratio is additive: $1 - St \approx 1 - St_{\mathrm{gr}} - St_{\mathrm{wr}}$. Supposing that the quality of grating substrate polishing is the same as the quality of polishing the optics used for writing the grating, we have $\overline{g^2} = \overline{w^2} = \sigma^2$ and $\overline{G_x^2} = \overline{W_x^2} = \overline{G_y^2} = \overline{W_y^2} = \Sigma^2$. We also assume that x and y are equivalent. Then it is readily found that

$$\frac{1 - St_{2,\mathrm{gr}}}{1 - St_{2,\mathrm{wr}}} = \frac{1}{2}\mathrm{tg}\beta N\lambda_{\mathrm{wr}}, \quad \frac{1 - St_{4,\mathrm{gr}}}{1 - St_{4,\mathrm{wr}}} = \frac{1}{2}\mathrm{ctg}\left(\frac{\alpha - \beta}{2}\right) N\lambda_{\mathrm{wr}}.$$

For typical compressor parameters, both ratios are $<<1$, that is, the imperfection of the optics used to write the grating exerts a greater influence. For example, for the 4TC and 4LC parameters proposed in Ref. [41] for the XCELS and SEL-100PW projects (Table 1), $St_{4,\mathrm{gr}}(\Sigma)$ and $St_{4,\mathrm{wr}}(\Sigma)$ are plotted in Figure 3, from which it is clear that $St_{4,\mathrm{gr}}(\Sigma) \approx St_{4,\mathrm{wr}}((2.5{-}3)\,\Sigma)$, that is, the requirements for the optics used to write the grating are approximately 2.5–3 times higher. The curves are plotted for $\lambda_{\mathrm{wr}} = 413$ nm; for $\lambda_{\mathrm{wr}} = 266$ nm this coefficient will be even 1.55 times larger.

From Equation (15) it is clear that u does not depend on N and the dependence of $\mathbf{U}$ on N is very weak. Consequently, $St_{\mathrm{wr},4}$ weakly depends on N, and $St_{\mathrm{wr},2}$ does not depend on it at all. Contrariwise, f and $\mathbf{F}$ and, hence, St_{gr}, depend on N. In Figure 4, $St_{\mathrm{gr}}(N)$ and $St_{\mathrm{wr}}(N)$ are plotted for four compressor configurations: 4TC, 4LC, 2TC and 2LC. For the TC, $\gamma = 0$ and the value of $|\alpha - \alpha_{\mathrm{L}}|$ for each N was chosen to be minimal, ensuring decoupling (grating G2 does not overlap the beam incident on grating G1). Analogously, for LC the angle γ was chosen to be minimal and $\alpha = \alpha_{\mathrm{L}}$. For all points in Figure 4 the distance between the gratings L corresponds to the group velocity dispersion of 4.4 ps^2. For identical Σ and σ, the values of $St_{\mathrm{gr}}(N)$ differ little from unity. Therefore, for clarity, the curves for $St_{\mathrm{gr}}(N)$ are plotted a factor of 10 larger for Σ (Figure 4(a)) and a factor of 5 larger for σ (Figure 4(b)) than for $St_{\mathrm{wr}}(N)$. This once again emphasizes that the contribution of h_{wr} is much larger than that of h_{gr}. As expected, St_{wr} (green symbols) is virtually independent of N, except for a small drop at large N in Figure 4(a). For the same quality of the optics,

https://doi.org/10.1017/hpl.2025.10047 Published online by Cambridge University Press

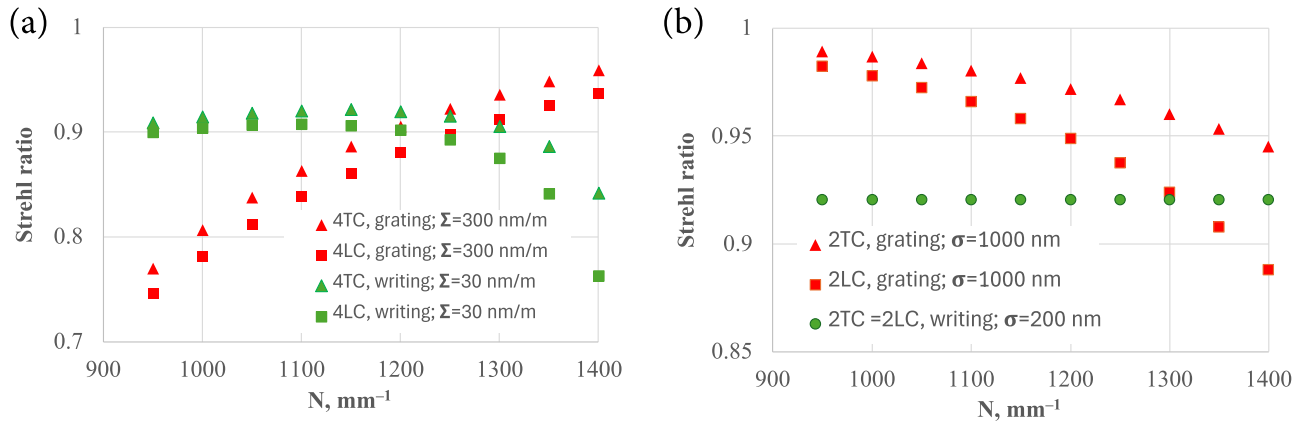

Figure 4. Here, $St_{gr}(N)$ (red) and $St_{wr}(N)$ (green) for 4TC and 4LC are plotted by Equation (25) (a); 4TC and 2TC are plotted by Equation (25) and 2LC is plotted by Equation (26) (b). The incidence angles α and γ as well as the distance between the gratings L are described in the text. For clarity, the curves for $St_{gr}(N)$ are plotted for larger values of distortion than for $St_{wr}(N)$: a factor of 10 for (a) and a factor of 5 for (b).

$St_{gr}(N) \approx 1$ and $St(N) \approx St_{wr}(N)$. However, if Equation (22) is met or quadratic components (defocus, vertical astigmatism and oblique astigmatism) dominate in h_{wr}, then $St_{wr}(N) \approx 1$ and $St(N) \approx St_{gr}(N)$. In this case, as can be seen from Figure 4, for 4TC and 4LC it is more advantageous to have large N, and for 2TC and 2LC small N. The comparison of TC and LC (triangles versus squares) shows that St is larger for TC, but the difference is insignificant, and for the two-grating compressor St_{wr} is the same for 2TC and 2LC (circles in Figure 4(b)).

4. Conclusion

The focal intensity (Strehl ratio St) depends on the grating surface profile $h_{gr}(x, y)$ and on the groove pattern imperfection $h_{wr}(x, y)$ – the function that, in turn, is determined by the total surface profile of the optics used for writing the holographic gratings. In the majority of cases, the influence of $h_{wr}(x, y)$ is much more significant, that is, the requirements for the quality of the surface of the optics used for inscribing the gratings are several times higher than for the quality of the grating surface.

When the grating is rotated by 180 degrees around its normal, $h_{wr}(x, y)$ (unlike $h_{gr}(x, y)$) changes its sign. By rotating the gratings and interchanging them it is possible to find an optimal variant for maximizing St.

The influence of all imperfections of all compressor gratings on St is described by one function $\Psi(x, y)$ that has the sense of the effective wavefront. The decrease in St is proportional to the squared rms of this function. The $\Psi(x, y)$ function is determined by the total distortions of gratings G2 and G3 for the four-grating compressor (Equation (14)) and of G1 and G2 for the two-grating compressor (Equation (13)), with the St decrease in the latter being much smaller, which is its undoubted advantage.

The number of grooves N almost does not affect the decrease in St due to groove pattern imperfection, but it influences the St decrease due to the imperfection of the grating surface. In four-grating compressors, St increases with increasing N, while in two-grating compressors it decreases. The comparison of the Treacy and Littrow compressors demonstrated that St is higher for the TC but the difference is insignificant.

In all cases the reduction of the pulse spectrum width $\Delta\omega$ proportionally reduces the requirements for the rms of both the surface of the gratings and the surface of the optics used for their writing.

References

1. C. Danson, J. Bromage, T. Butcher, J.-C. Chanteloup, E. Chowdhury, A. Galvanauskas, L. Gizzi, C. Haefner, J. Hein, D. Hillier, N. Hopps, Y. Kato, E. Khazanov, R. Kodama, G. Korn, R. Li, Y. Li, J. Limpert, J. Ma, C. H. Nam, D. Neely, D. Papadopoulos, R. Penman, L. Qian, J. Rocca, A. Shaykin, C. Siders, C. Spindloe, S. Szatmári, R. Trines, J. Zhu, P. Zhu, and J. Zuegel, High Power Laser Sci. Eng. **7**, e54 (2019).
2. Z. Li, Y. Leng, and R. Li, Laser Photonics Rev. **7**, 2100705 (2022).
3. P. Tournois, Opt. Commun. **140**, 245 (1997).
4. V. Samarkin, A. Alexandrov, G. Borsoni, T. Jitsuno, P. Romanov, A. Rukosuev, and A. Kudryashov, High Power Laser Sci. Eng. **4**, e4 (2016).
5. C. Dorrer and J. Bromage, Opt. Express **16**, 3058 (2008).
6. J. Bromage, C. Dorrer, and R. K. Jungquist, J. Opt. Soc. Am. B **29**, 1125 (2012).
7. S. Roeder, Y. Zobus, C. Brabetz, and V. Bagnoud, High Power Laser Sci. Eng. **10**, e34 (2022).
8. V. Bagnoud and F. Salin, J. Opt. Soc. Am. B **16**, 188 (1999).
9. B. Webb, C. Feng, C. Dorrer, C. Jeon, R. G. Roides, S. Bucht, and J. Bromage, Opt. Express **32**, 12276 (2024).
10. B. Webb, C. Dorrer, S.-W. Bahk, C. Jeon, R. G. Roides, and J. Bromage, Appl. Opt. **63**, 4615 (2024).
11. Z. Li, S. Tokita, S. Matsuo, K. Sueda, T. Kurita, T. Kawasima, and N. Miyanaga, Opt. Express **25**, 21201 (2017).
12. Z. Li, J. Liu, Y. Xu, Y. Leng, and R. Li, Opt. Express **30**, 41296 (2022).
13. A. Vyatkin and E. Khazanov, Opt. Express **32**, 39394 (2024).
14. Z. Li and J. Kawanaka, Opt. Express **27**, 25172 (2019).
15. Z. Li and N. Miyanaga, Opt. Express **26**, 8453 (2018).

https://doi.org/10.1017/hpl.2025.10047 Published online by Cambridge University Press

16. V. Leroux, T. Eichner, and A. R. Maier, Opt. Express **28**, 8257 (2020).
17. J. Qiao, J. Papa, and X. Liu, Opt. Express **23**, 25923 (2015).
18. Z. Li, K. Tsubakimoto, H. Yoshida, Y. Nakata, and N. Miyanaga, Appl. Phys. Express **10**, 102702 (2017).
19. J. Liu, X. Shen, Z. Si, C. Wang, C. Zhao, X. Liang, Y. Leng, and R. Li, Opt. Express **28**, 22978 (2020).
20. J. Liu, X. Shen, S. Du, and R. Li, Opt. Express **29**, 17140 (2021).
21. E. Khazanov, High Power Laser Sci. Eng. **12**, e85 (2024).
22. F. Bienert, C. Röcker, T. Graf, and M. A. Ahmed, Opt. Express **31**, 19392 (2023).
23. E. Khazanov, Opt. Express **32**, 46310 (2024).
24. F. Bienert, C. Röcker, T. Dietrich, T. Graf, and M. A. Ahmed, Opt. Express **31**, 40687 (2023).
25. N. Bonod and J. Neauport, Adv. Opt. Photonics **8**, 156 (2016).
26. E. B. Treacy, IEEE J. Quantum Electron. **QE-5**, 454 (1969).
27. X. Shen, S. Du, W. Liang, P. Wang, J. Liu, and R. Li, Appl. Phys. B **128**, 159 (2022).
28. E. Khazanov, High Power Laser Sci. Eng. **11**, e93 (2023).
29. S. Du, X. Shen, W. Liang, P. Wang, J. Liu, and R. Li, High Power Laser Sci. Eng. **11**, e4 (2023).
30. M. Trentelman, I. N. Ross, and C. N. Danson, Appl. Opt. **36**, 8567 (1997).
31. K. Osvay and I. N. Ross, Opt. Commun. **105**, 271 (1994).
32. G. Kalinchenko, S. Vyhlidka, D. Kramer, A. Lererc, and B. Rus, Proc. SPIE **9626**, 96261R (2015).
33. D. L. Smith, S. L. Erdogan, and T. Erdogan, Appl. Opt. **62**, 3357 (2023).
34. Y. Han, H. Cao, F. Kong, Y. Jin, and J. Shao, High Power Laser Sci. Eng. **11**, e60 (2023).
35. L. Li, J. Opt. Soc. Am. A **38**, 426 (2021).
36. K. Wei and L. Li, Opt. Lett. **46**, 4626 (2021).
37. Š. Vyhlídka, P. Trojek, D. Kramer, D. Peceli, F. Batysta, J. Bartoníček, J. Hubáček, T. Borger, R. Antipenkov, E. Gaul, T. Ditmire, and B. Rus, Proc. SPIE **11034**, 1103409 (2019).
38. C. M. Werle, C. Braun, T. Eichner, T. Hulsenbusch, G. Palmer, and A. R. Maier, Opt. Express **31**, 37437 (2023).
39. E. Khazanov, Laser Phys. Lett. **20**, 125001 (2023).
40. D. E. Kiselev, A. A. Kochetkov, I. V. Yakovlev, and E. A. Khazanov, Appl. Opt. **63**, 9146 (2024).
41. E. Khazanov, High Power Laser Sci. Eng. **12**, e36 (2024).
42. H. Huang and T. Kessler, Opt. Lett. **32**, 1854 (2007).
43. C. Wang, D. Wang, Y. Xu, and Y. Leng, Opt. Commun. **507**, 127613 (2022).

https://doi.org/10.1017/hpl.2025.10047 Published online by Cambridge University Press